

# Thermal UV treatment on SU-8 polymer for integrated optics

Xi-Bin Wang,<sup>1</sup> Jian Sun,<sup>1</sup> Chang-Ming Chen,<sup>1</sup> Xiao-Qiang Sun,<sup>1</sup> Fei Wang,<sup>1</sup> and Da-Ming Zhang<sup>1,\*</sup>

<sup>1</sup> State Key Laboratory on Integrated Optoelectronics, College of Electronic Science and Engineering, Jilin University, 2699 Qianjin Street, Changchun 130012, China

\*zhangdm@jlu.edu.cn

**Abstract:** We report a simple and low-cost method to fabricate SU-8-based polymer waveguide devices. The influence of hard-baking temperature on SU-8 polymer treated with or without UV radiation was investigated in detail. Based on these properties, the straight type, Y branch type, March-Zehnder (M-Z) type and  $1 \times 4$  splitter waveguides were successfully fabricated. And a polymeric thermal-optic (TO) switch with M-Z type waveguide was also fabricated by this method. The device exhibits low power consumption of less than 6.4 mW, fast rise time of about 149.3  $\mu$ s and fast fall time of about 139.3  $\mu$ s. The experimental results showed that this method can bypass the need for complex lithography and provide high resolution and fine waveguide quality desired for TO switches as well as other planar lightwave devices.

©2014 Optical Society of America

**OCIS codes:** (160.5335) Photosensitive materials; (260.7190) Ultraviolet; (160.4760) Optical properties; (130.5460) Polymer waveguides; (130.3120) Integrated optics devices.

---

## References and links

1. M. Wang, J. Hiltunen, C. Liedert, S. Pearce, M. Charlton, L. Hakalahti, P. Karioja, and R. Myllylä, "Highly sensitive biosensor based on UV-imprinted layered polymeric-inorganic composite waveguides," *Opt. Express* **20**(18), 20309–20317 (2012).
2. B. Y. Fan, F. Liu, Y. X. Li, Y. D. Huang, Y. Miura, and D. Ohnishi, "Refractive index sensor based on hybrid coupler with short-range surface plasmon polariton and dielectric waveguide," *Appl. Phys. Lett.* **100**(11), 111108 (2012).
3. S. W. Kwon, W. S. Yang, H. M. Lee, W. K. Kim, G. S. Son, D. H. Yoon, S.-D. Lee, and H.-Y. Lee, "The fabrication of polymer-based evanescent optical waveguide for biosensing," *Appl. Surf. Sci.* **255**(10), 5466–5470 (2009).
4. Y. Enami, D. Mathine, C. T. DeRose, R. A. Norwood, J. Luo, A. K.-Y. Jen, and N. Peyghambarian, "Hybrid electro-optic polymer/sol-gel waveguide directional coupler switches," *Appl. Phys. Lett.* **94**(21), 213513 (2009).
5. K.-L. Lei, C.-F. Chow, K.-C. Tsang, E. N. Y. Lei, V. A. L. Roy, M. H. W. Lam, C. S. Lee, E. Y. B. Pun, and J. Li, "Long aliphatic chain coated rare-earth nanocrystal as polymer-based optical waveguide amplifiers," *J. Mater. Chem.* **20**(35), 7526–7529 (2010).
6. A. Kocabas and A. Aydinli, "Polymeric waveguide Bragg grating filter using soft lithography," *Opt. Express* **14**(22), 10228–10232 (2006).
7. B. Bêche, P. Papet, D. Debarnot, E. Gaviot, J. Zyss, and F. Poncin-Epaillard, "Fluorine plasma treatment on SU-8 polymer for integrated optics," *Opt. Commun.* **246**(1–3), 25–28 (2005).
8. X. Wang, J. Meng, X. Sun, T. Yang, J. Sun, C. Chen, C. Zheng, and D. Zhang, "Inductively coupled plasma etching to fabricate sensing window for polymer waveguide biosensor application," *Appl. Surf. Sci.* **259**(15), 105–109 (2012).
9. L. Jiang, K. P. Gerhardt, B. Myer, Y. Zohar, and S. Pau, "Evanescent-wave spectroscopy using an SU-8 waveguide for rapid quantitative detection of biomolecules," *J. Microelectromech. Syst.* **17**(6), 1495–1500 (2008).
10. B. Yang, L. Yang, R. Hu, Z. Sheng, D. Dai, Q. Liu, and S. He, "Fabrication and characterization of small optical ridge waveguides based on SU-8 polymer," *J. Lightwave Technol.* **27**(18), 4091–4096 (2009).
11. X. Zhai, J. Li, S. Liu, X. Liu, D. Zhao, F. Wang, D. Zhang, G. Qin, and W. Qin, "Enhancement of 1.53  $\mu$ m emission band in NaYF<sub>4</sub>:Er<sup>3+</sup>, Yb<sup>3+</sup>, Ce<sup>3+</sup> nanocrystals for polymer-based optical waveguide amplifiers," *Mater. Express* **3**(2), 270–277 (2013).
12. C. Liu, "Recent developments in polymer MEMS," *Adv. Mater.* **19**(22), 3783–3790 (2007).

13. M. Nordström, D. A. Zauner, A. Boisen, and J. Hübner, "Single-mode waveguides with SU-8 polymer core and cladding for MOEMS applications," *J. Lightwave Technol.* **25**(5), 1284–1289 (2007).
14. Y. Wang, J.-H. Pai, H.-H. Lai, C. E. Sims, M. Bachman, G. P. Li, and N. L. Allbritton, "Surface graft polymerization of SU-8 for bio-MEMS application," *J. Micromech. Microeng.* **17**(7), 1371–1380 (2007).
15. C.-S. Huang and W.-C. Wang, "Large-core single-mode rib SU8 waveguide using solvent-assisted microcontact molding," *Appl. Opt.* **47**(25), 4540–4547 (2008).
16. B. Yang, Y. P. Zhu, Y. Q. Jiao, L. Yang, Z. Sheng, S. He, and D. Dai, "Compact arrayed waveguide grating devices based on small SU-8 strip waveguides," *J. Lightwave Technol.* **29**(13), 2009–2014 (2011).
17. C. Chen, X. Sun, D. Zhang, Z. Shan, S.-Y. Shi, and D. Zhang, "Dye-doped polymeric planar waveguide devices based on a thermal UV-bleaching technique," *Opt. Laser Technol.* **41**(4), 495–498 (2009).
18. R. Singhal, M. N. Satyanarayan, and S. Pal, "Fabrication of monomode channel waveguides in photosensitive polymer on optical adhesive," *Opt. Eng.* **50**(9), 094601 (2011).
19. B. H. Ong, X. Yuan, and S. C. Tjin, "Adjustable refractive index modulation for a waveguide with SU-8 photoresist by dual-UV exposure lithography," *Appl. Opt.* **45**(31), 8036–8039 (2006).
20. B. H. Ong, X. C. Yuan, S. H. Tao, and S. C. Tjin, "Photothermally enabled lithography for refractive-index modulation in SU-8 photoresist," *Opt. Lett.* **31**(10), 1367–1369 (2006).
21. M. K. Gunde, N. Hauptman, M. Maček, and M. Kunaver, "The influence of hard-baking temperature applied for SU8 sensor layer on the sensitivity of capacitive chemical sensor," *Appl. Phys., A Mater. Sci. Process.* **95**(3), 673–680 (2009).
22. B. Y. Shew, C. H. Kuo, Y. C. Huang, and Y. H. Tsai, "UV-LIGA interferometer biosensor based on the SU-8 optical waveguide," *Sens. Actuators A Phys.* **120**(2), 383–389 (2005).
23. L. Gao, J. Sun, X. Sun, C. Kang, Y. Yan, and D. Zhang, "Low switching power 2×2 thermal-optic switch using direct ultraviolet photolithography process," *Opt. Commun.* **282**(20), 4091–4094 (2009).
24. A. M. Al-Hetar, A. B. Mohammad, A. S. M. Supa'at, and Z. A. Shamsan, "MMI-MZI polymer thermal-optic switch with a high refractive index contrast," *J. Lightwave Technol.* **29**(2), 171–178 (2011).
25. Z. Cao, Y. Yan, J. Meng, L. Jin, and D. Zhang, "Low power consumption thermal-optic switch based on DRI/PMMA," *Microw. Opt. Technol. Lett.* **54**(9), 2163–2165 (2012).

## 1. Introduction

Integrated optics and passive waveguides are increasingly being used in sensors applications [1–3] and optical telecommunication systems such as switches, amplifiers, wavelength filters, and splitters [4–6]. In the past two decades, various passive polymer materials have been used to fabricate waveguide devices for bio-sensing and telecommunication applications because of their low cost, high thermo-optic coefficients, and simple processing steps. Examples include polyimide, polymethylmethacrylate (PMMA), polydimethylsiloxane (PDMS) and epoxy novolak resin [7]. Among various polymer material, SU-8 is a promising candidate for integrated optics in sensors and telecommunication applications and has been widely used in polymer waveguide devices [8–11]. Besides being an epoxy-based negative photoresist with high aspect ratio, good self-leveling capability and dimensional control, polymer SU-8 also play a key role in micro-electro-mechanical systems (MEMS), micro-optic-electro-mechanical systems (MOEMS) and bio-micro-electro-mechanical systems (Bio-MEMS) [12–14]. Moreover, it exhibits excellent optical properties, such as relative high refractive index and low loss over a wide wavelength range [10]; thus it is a suitable material for integrated optical microcomponents, e.g., waveguide elements [9,15,16].

Single-mode and multi-mode polymer waveguide structures can be readily formed using standard semiconductor fabrication technology. Several techniques have been reported for the fabrication of polymer waveguides, including reactive ion etching (RIE), ion-implantation, ultra-violet (UV) laser beam scanning, and electron-beam lithography [17]. However, these techniques are high cost and often contain many complicated steps in the fabrication process. Polymer planar waveguide technology tends out to be a cost effective technology. For the fabrication of SU-8 waveguides, though the conventional UV photolithography and wet-etching method can simplify the processing steps, this fabricating process is still relatively complicated [16,18]. In fact, SU-8 is a photosensitive polymer, and its refractive index is sensitive to the thermal UV processing parameters. The SU-8 polymeric waveguides can be fabricated by thermal UV bleaching instead of wet-etching method.

Ong *et al.* [19,20] has fabricated the SU-8 waveguide by dual-UV exposure lithography method, they altered refractive index of SU-8 photoresist by changing the preexposure baking

time. Different from their work, we alter the refractive index by changing the hard-baking temperature for the exposed and unexposed film. By this means, the refractive index contrast can be adjusted with a wide range, and the waveguide fabricating process is relative simpler. In this work, we bypass the need for complex lithography by utilizing a simple thermal UV bleaching method to fabricate polymeric channel waveguides with a photosensitive polymer SU-8. The influence of hard-baking temperature on SU-8 polymer treated with or without UV bleaching were studied in detail, including the surface morphology and refractive index. Fourier transform infrared spectroscopy was also introduced to analyze the effect of hard-baking temperature on SU-8 polymer with or without UV bleaching. Finally, the straight type, Y branch type, March-Zehnder (M-Z) type and  $1 \times 4$  splitter waveguides were successfully fabricate by this method. And a polymeric thermal-optic (TO) switch with M-Z type waveguide was also fabricated. The device presents a low power consumption and a fast response time.

## 2. Experimental

### 2.1. Material

SU-8 2005 photoresist was used in this study. Example structure of a molecule with eight epoxy groups as it might be present in the SU-8 2005 resin, and the structure of the monomer unit is shown in Fig. 1. Each monomer unit has 8 functional groups (epoxy rings), giving the commercial name of the chemical, the SU-8 [21]. SU-8 2005 has very high optical transmission for the wavelength range above 360 nm, which makes it ideally suited for imaging near vertical sidewalls in very thick films.

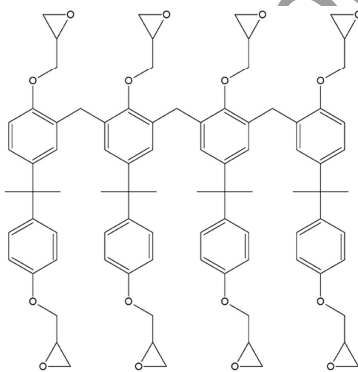


Fig. 1. The molecular structure of SU-8 monomer unit.

### 2.2. Thermal UV treatment and sample preparation

The films were prepared to measure the characteristics of SU-8 2005 polymer with or without thermal UV treating process. The detailed fabrication process of the films is as follows. Firstly, the SU-8 2005 polymer were spin-coated on the clean silicon substrates and pre-baked at 65 °C for 15 min, 90 °C for 20 min in oven. Next, some of the coated wafers were exposed to UV light from a mercury discharge lamp with a peak emission at 365 nm wavelength and an irradiance of 15 mW/cm<sup>2</sup> for 15 s, and then the wafers with exposed and unexposed film were post-baked at 65 °C for 15 min, 95 °C for 20 min. Finally, the wafers with exposed and unexposed film were hard-baked at 95 °C, 120 °C, 140 °C, and 170 °C, respectively, for 10 min.

### 3. Results and discussion

#### 3.1. Surface morphology

The surface morphology of the sample was firstly examined using an OLYMPUS DSX500 optical microscope. As shown in Fig. 2(a), a group of waveguides could be identified from the image. The three waveguides revealed the straight, the Y-branch and the middle sections of the M-Z waveguides, which were induced by thermal UV bleaching method. The inset of Fig. 2(a) is a magnified figure of the selected M-Z waveguide (in the middle). The surface profile of the waveguide was also characterized with a CSPM 500 atomic force microscope (AFM) operated in the contact mode. Figure 2(b) shows a 3D view of the waveguide surface. The height profile of the white line in Fig. 2(c) shows that the decrease in the thickness of the patterned area is about 400 nm [Fig. 2(d)].

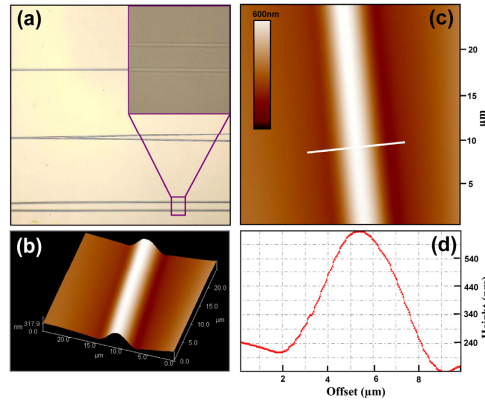


Fig. 2. Surface morphologies of the sample. (a) Optical microscope image of the M-Z waveguides, the inset is a magnified figure of the selected M-Z waveguide (in the middle); (b) 3D-AFM image of the waveguide surface; (c) 2D-AFM image of the waveguide surface; (d) The height profile of the white line.

#### 3.2. Refractive index

In the experiment, we also found that the thermal UV treating process not only slightly reduced the thickness of the SU-8 film, but also changed the refractive index of the polymer. As the hard-baking temperature increased, a significant change in the refractive index of the polymer occurred in the exposed and unexposed films. The refractive indices of the films were measured at 1550 nm wavelength using an M-2000 UI variable angle incidence spectroscopic ellipsometer. Figure 3 shows the indices of the exposed and unexposed films as a function of hard-baking temperature. It is clear that, as the temperature increases, the material refractive index decreases in the exposed region, while increases in the unexposed region. This phenomenon can be indicated by the Lorentz-Lorentz equation:

$$\frac{n^2 - 1}{n^2 + 2} = \frac{4\pi N}{3M\epsilon} \rho\beta, \quad (1)$$

where  $N$  is the Avogadro number,  $M$  is the molecular weight of the polymer repeat unit,  $\epsilon$  is the permittivity of free space,  $\rho$  is the density, and  $\beta$  is the polarizability of the molecules [19,20]. In the exposed film, with the increasing of hard-baking temperature, the degree of cross-linking and polymerization become more and more thorough, and molecular weight  $M$  of the polymer is also increased [17,22]. According to Lorentz-Lorentz equation, the refractive index  $n$  would be decreased. In the unexposed film, the molecular weight  $M$  was almost constant, and the increases in refractive index is mainly due to the increase in the

density  $\rho$ , which is caused by the further evaporation of the solvent [19,20]. However, In the whole hard-baking process, the increase of the molecular weight occupies the main position, so there is a decrease in the exposed region and an increase in the unexposed region.

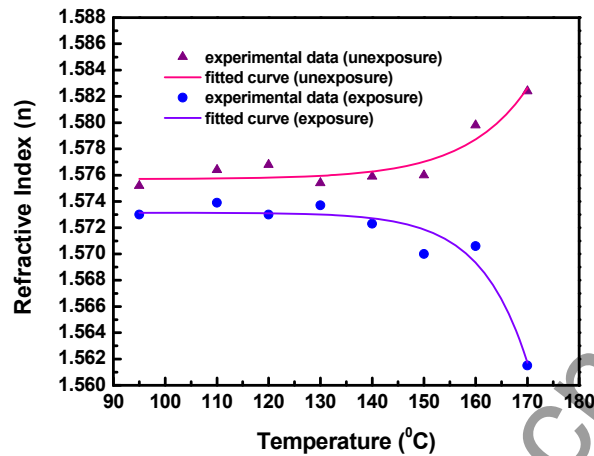


Fig. 3. Curves of refractive indices of the exposed and unexposed films at 1550 nm wavelength versus the hard-baking temperatures.

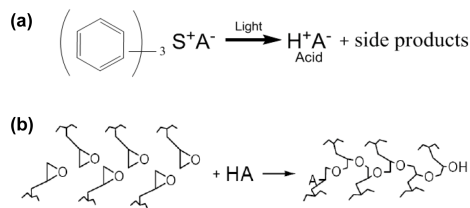


Fig. 4. The detailed reaction yielded by exposing and hard-baking the photosensitive polymer SU-8 2005. (a) Illustration of the UV-induced reaction of SU-8 2005; (b) Illustration of the temperature-induced reaction of SU-8 2005.

In fact, after pre-baking acids were formed during the UV exposure of the film, and they catalyze cross-linking and polymerization of the film during the hard-baking process. The detailed reaction yielded by exposing and hard-baking the photosensitive polymer SU-8 2005 to UV light have been illustrated in Fig. 4. Under catalyzing of the formed acid in the exposed areas, the SU-8 polymer begin to cross-link and polymerize. Furthermore, with the hard-baking temperature increasing, the degree of cross-linking and polymerization become more and more thorough. This reaction can be monitored by IR spectroscopy. IR spectra of the hard-baked samples with or without UV radiation at different temperature were taken on an AVATAR 360 FTIR spectrometer in the  $450\text{-}2150\text{ cm}^{-1}$  interval. As shown in Fig. 5, IR vibrations of epoxy ring give characteristic peaks at  $1250$ ,  $830$ , and  $915\text{ cm}^{-1}$ . The chain-terminating group is involved in cross-linking and polymerization process of the polymer, and its vibrations therefore can reflect the information about the state of the polymer. The peak at  $915\text{ cm}^{-1}$  corresponds to stretching of  $\text{CH}_2$  group on epoxy ring, and its intensity can be used to reflect the degree of polymerization of the SU-8 polymer [21]. As shown in Fig. 5(a), with the hard-baking temperature increasing on the exposed films, the intensity of the  $915\text{ cm}^{-1}$  peak becomes smaller and smaller and is almost completely absent at  $170\text{ }^\circ\text{C}$ . The disappearance of the peak also clearly indicates that a almost thorough cross-linking of the SU-8 polymer occurs. While the other two characteristic peaks of the epoxy ring,  $830$  and  $1250\text{ cm}^{-1}$ , correspond to symmetric and asymmetric stretching vibrations of C-O-C group in mono-substituted epoxy rings, respectively. Both peaks remain constant in IR spectrum of the

SU-8 layer up to much higher temperatures than the  $915\text{ cm}^{-1}$  peak [21]. However, with the hard-baking temperature increasing on the unexposed films, the intensity of the three characteristic peaks,  $1250$ ,  $830$ , and  $915\text{ cm}^{-1}$ , seem to not change [Fig. 5(b)]. It can be explained that the SU-8 film can't cross-link and polymerize without the catalyzing of the formed acid, which is produced under the UV exposure.

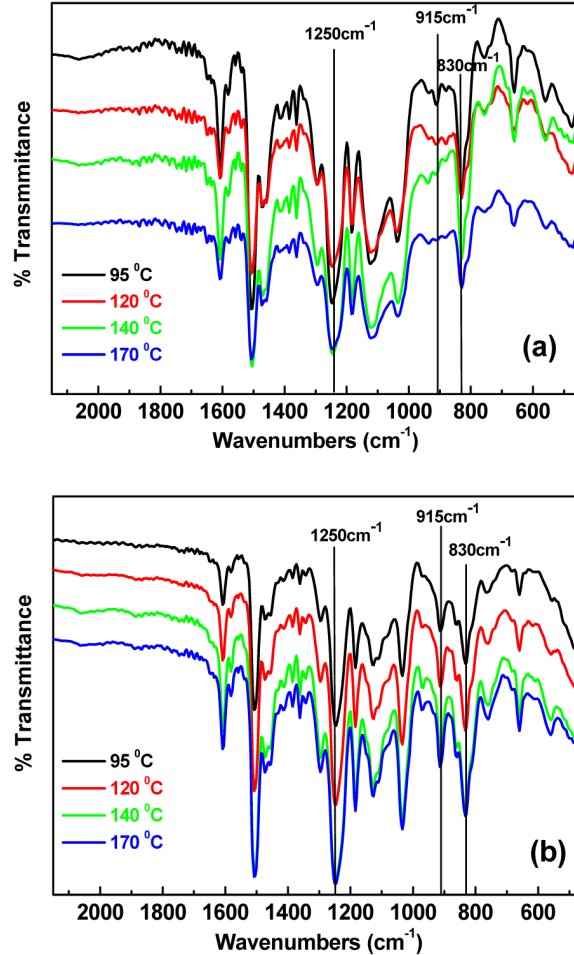


Fig. 5. FTIR spectra of (a) exposed and (b) unexposed SU-8 2005 films at various hard-baking temperatures.

### 3.3. Waveguide fabrication and application

Based on the above characteristics, a simple fabrication process was designed for fabricating the polymeric channel waveguides using SU-8 2005 polymer. The detailed fabrication process is shown in Fig. 6(a)-6(e). Firstly, SU-8 2005 was spin-coated on a silicon substrate with a  $2.5\text{ }\mu\text{m}$  of silicon dioxide layer at a spinning rate of  $4000\text{ r/min}$ , and pre-baked at  $65\text{ }^\circ\text{C}$  for  $15\text{ min}$ ,  $90\text{ }^\circ\text{C}$  for  $20\text{ min}$  to form a  $3\text{ }\mu\text{m}$  film. Next, the coated wafer was exposed through a photomask to UV light from a mercury discharge lamp with a peak emission at  $365\text{ nm}$  wavelength and an irradiance of  $15\text{ mW/cm}^2$  for  $15\text{ s}$  and post-baked at  $65\text{ }^\circ\text{C}$  for  $15\text{ min}$  then  $95\text{ }^\circ\text{C}$  for  $20\text{ min}$ . After that, the sample was hard-baked at  $170\text{ }^\circ\text{C}$  for  $10\text{ min}$ , then the waveguides will be obtained easily. Finally,  $2\text{ }\mu\text{m}$  poly-methyl-methacrylate (PMMA) was spin-coated on them as the upper-cladding. To measure the waveguides performance, the light beam (at  $1550\text{ nm}$ ) produced by a tunable semiconductor laser (TSL-210, Santec) was

coupled directly into the input port by a standard single mode fiber (SMF), and the output light beam was collected by a lens and coupled into a detector. The near-field patterns can be observed by an infrared charge-coupled device (CCD) camera and displayed on a video monitor. A fiber-optic polarization controller was used to adjust the input polarization to TM. Figure 7 shows the near-field guided-mode patterns of straight type, Y branch type, M-Z type and  $1 \times 4$  splitter waveguides. At the same time, cut-back measurements at 1550 nm were made to measure the propagation loss of the waveguides. To increase the accuracy of the measurement, several waveguides were measured at each length. The 5- $\mu\text{m}$ -wide straight waveguide has a propagation loss of 1.76 dB/cm. And the loss calculated for Y-splits was also obtained, which was about 0.22 dB/split.

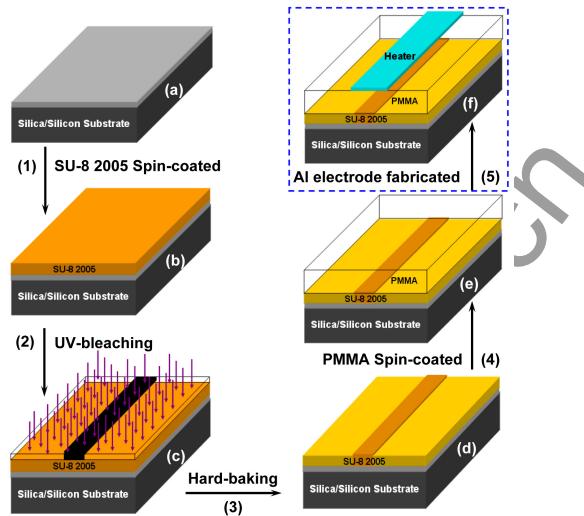


Fig. 6. Fabrication process of waveguide device.

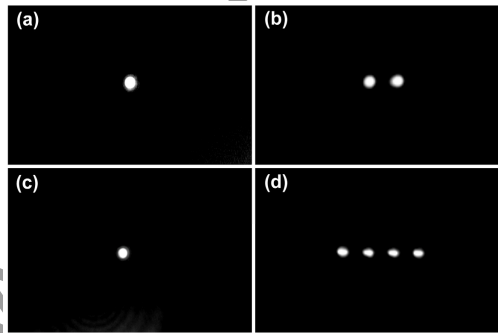


Fig. 7. Near-field guided-mode patterns. (a) straight type; (b) Y branch type; (c) M-Z type; (d)  $1 \times 4$  splitter waveguide at 1550 nm wavelength.

After successfully fabricating the M-Z type waveguides, we evaporated 300-nm-thick aluminium (Al) layer on top of upper-cladding via thermal evaporation to fabricate polymeric thermal-optic (TO) switch. Then 8- $\mu\text{m}$ -width heating electrodes were patterned by conventional photolithography and wet etching method [Fig. 6(f)]. To measure the switch performance, input power (1 mW@1550 nm) from the SMF was coupled into the switch. The insertion loss was obtained to be less than 10.5 dB, including the coupling loss, transmission loss and excess loss. When the driving power is applied on the heating electrode, the relative output power is shown in Fig. 8. From this figure, we see that the switching power of the switch was measured to be 6.4 mW, and the extinction ratio is roughly 18.9 dB. The insets of

Fig. 8 show the near-field guided-mode of the device at 1550 nm wavelength under ON- and OFF-state, respectively. Using a rectangular wave signal to drive the switch, the dynamical performance was expressed by the rise and fall times of 149.3  $\mu$ s and 139.3  $\mu$ s, respectively, as shown in Fig. 9.

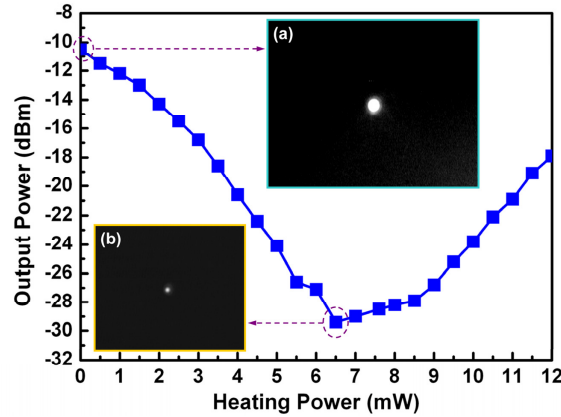


Fig. 8. Measured curve of output power versus heating power. The insets show the near-field guided-mode of the device at 1550 nm wavelength under (a) ON-state and (b) OFF-state.



Fig. 9. Switching response of the TO switch on a 0.2 KHz rectangular wave. The upper is the driving voltage signal, and the lower is the switching response.

As a comparison, Table 1 shows the performances of this hybrid silica/polymer TO switch and those of other reported all-polymer TO switches [23–25]. It is clear that, compared with the other three kinds of switches, this fabricated switch possesses acceptable performances, including both power consumption and response time. The reason can be explained as below. First, the TO coefficient of the core polymer SU-8 is large, which is helpful to reduce power consumption. Second, the thickness of the PMMA upper-cladding and silica under-cladding are optimally decreased to the minimum value, which is helpful for heat releasing from the heating electrodes to the silicon heat sink and shortening the response time. Moreover, the silica under-cladding has a relative larger thermal conductivity, which is also useful for heat releasing from the core to the silicon heat sink.

**Table 1. Comparisons among the performances of this TO switch and those of other polymer TO switches**

| References | Material       | Power consumption<br>(mW) | Rise time<br>( $\mu$ s) | Fall time<br>( $\mu$ s) |
|------------|----------------|---------------------------|-------------------------|-------------------------|
| Ref. 23    | Polymer        | 7.5                       | 320                     | 400                     |
| Ref. 24    | Polymer        | 1.85                      | 300                     | 700                     |
| Ref. 25    | Polymer        | 13                        | 459.3                   | 465.5                   |
| This paper | Polymer/Silica | 6.4                       | 149.3                   | 139.3                   |

#### 4. Conclusions

In summary, a simple and low-cost method has been successfully used to fabricate polymer waveguide devices. The influence of hard-baking on SU-8 polymer have been investigated in detail by using image analysis, Fourier transform infrared spectroscopy and refractive index measurement. The films treated with or without UV light showed sensitive to the hard-baking temperature. With the increasing of hard-baking temperature, a significant change in the refractive index and surface morphology occurs in the exposed and unexposed films. Based on these properties, the straight type, Y branch type, M-Z type and  $1 \times 4$  splitter waveguides were successfully fabricated. And a polymeric TO switch with M-Z type waveguide was also fabricated by this method. The device exhibits low power consumption of less than 6.4 mW, fast rise time of about 149.3  $\mu$ s and fast fall time of about 139.3  $\mu$ s. The experimental results showed that this method can bypass the need for complex lithography and therefore reduces the number of processing steps. This method is also compatible with current silicon microprocessing techniques and could be implemented into large-scale processing line.

#### Acknowledgments

This work was supported by the NSFC (Grant Nos. 61177027, 61107019, 61205032, and 61261130586).